Materials Letters 271 (2020) 127791

Contents lists available at ScienceDirect

Materials Letters

journal homepage: www.elsevier.com/locate/mlblue

Microstructural and mechanical characteristics of 308L stainless steel manufactured by gas metal arc welding-based additive manufacturing

Van Thao Le [a,b,*], Dinh Si Mai [b]

[a] Institute of Research and Development, Duy Tan University, Da Nang 550000, Viet Nam
[b] Advanced Technology Center, Le Quy Don Technical University, Hanoi, Viet Nam

ARTICLE INFO

Article history:
Received 17 March 2020
Received in revised form 30 March 2020
Accepted 6 April 2020
Available online 7 April 2020

Keywords:
Additive manufacturing
Gas metal arc welding
Austenitic stainless steel
Microstructure
Phase transformation
Mechanical properties

ABSTRACT

In this paper, gas metal arc welding-based additive manufacturing (GMAW-AM) was used to build thin-walled 308L stainless steel parts. The microstructural and mechanical characteristics of the built thin walls were investigated. The results show that the GMAW-AM thin-walled 308L is dominantly composed of columnar dendrites, which grow along the build direction when increasing the number of depositing layers. The microstructure of the GMAW-AM thin-walled 308L mainly consists of two phases: a small amount of δ ferrite phases displayed within γ austenite dendrites. The microhardness of built materials ranges from 155 ± 1.20 $HV_{0.1}$ to 169 ± 5.67 $HV_{0.1}$. The average ultimate tensile strength (UTS), yield strength (YS) and elongation (EL) of the GMAW-AM thin-walled 308L in the vertical direction are 531.78 ± 4.52 MPa, 343.67 ± 7.53 MPa, and 39.58 ± 1.38%, respectively, which are obviously lower than those in the horizontal direction (UTS: 552.95 ± 4.96 MPa, YS: 352.69 ± 8.12 MPa, and EL: 54.13 ± 1.29%).

1. Introduction

Wire arc additive manufacturing (WAAM) using welding arc as the heat source to melt and deposit metallic wire layer-by-layer to form components has received much attention because of its high deposition rate and utilization efficiency of materials. The welding arc in WAAM can be gas tungsten arc welding (GTAW), gas metal arc welding (GMAW), and plasma arc welding (PAW) [1]. WAAM has been extensively investigated for the manufacture of components made of aluminum and titanium alloys in military and aerospace industries [2,3]. Concerning the manufacture of steel components by WAAM, most of the published works used low-carbon [4] and austenitic stainless steels such as 316L [5] and 304 [6]. For instance, Haden et al. [6] studied the microstructural and mechanical properties of both stainless steel (304) and mild steel (ER70S) manufactured by the GMAW-AM process. Chen et al. [7] investigated the microstructure and mechanical properties of 316L components built by GMAW-AM. Until now, limited works study the manufacture of 308L steel by WAAM. 308L is an austenitic stainless steel, which is widely used in gas, oil, and mining, as well as automobile industries because of its lower level of carbon. Some authors have considered 308L and 308LSi stainless steels as studied materials in GTAW-AM [8] and laminar plasma-based AM [9]. Very few studies reported the microstructural and mechanical properties of 308L parts manufactured by the GMAW-AM process. Therefore, this study aims at investigating the microstructural and mechanical properties of thin-walled 308L manufactured by the GMAW-AM process.

2. Materials and methods

The commercial GM-308L stainless steel wire with diameter of 1 mm (supplied by Kim Tin Corporation of Vietnam) was used to build the thin-walled samples on SS400 steel plates with dimensions of 200 mm × 100 mm × 10 mm by an industrial GMAW robot (Panasonic TA1400) according to the WAAM process. First thin-walled sample with dimensions of 20 mm in height and 100 mm in length was built for observing the microstructure and microhardness of built materials. Second thin-walled sample with dimensions of 100 mm in height and 220 mm in length was built for the tensile tests. All thin-walled samples were built by using the alternating deposition direction strategy and the same process parameters, including welding current of 120 A, voltage of 20 V and travel speed of 400 mm/min. A gas of 99.99% argon with a constant rate of 15 L/min was used for the shielding purpose during the build of thin-walled samples.

The chemical compositions of GMAW-AM thin-walled 308L were analyzed using a thermo Scientific Spectrometer, as shown

* Corresponding author at: Advanced Technology Center, Le Quy Don Technical University, Hanoi, Viet Nam.
E-mail address: thaomta@gmail.com (V.T. Le).

https://doi.org/10.1016/j.matlet.2020.127791
0167-577X/

in Table 1. It is found that the percentage of the main elements of built thin-walled 308L fall in the value range of GM-308L wire given by the manufacturer.

The microstructure of GMAW-AM thin-walled 308L was observed by an optical microscope on the grinded and chemically etched cross section of the first wall (Fig. 1a). The microhardness of built materials was measured by a Vickers microhardness tester with a load of 980.7 mN and a dwell time of 15 s applied for each indentation.

Three tensile specimens in each vertical or horizontal direction were extracted from the second thin-walled sample. The dimensions of each tensile specimen were designed according to ASTM E8M-13 standard. All tensile tests were performed on a tensile test machine with a displacement rate of 20 mm/min and at room temperature.

3. Results and discussion

Fig. 1a reveals an overall structure of a cross-section of GMAW-AM thin-walled 308L. It is observed that the thin wall was successfully built with no obvious defects such as cracks, pores, and incomplete fusion between the deposited layers. The structure of

Table 1
Chemical compositions of 308L austenitic stainless steel (in wt. %).

Element	Cr	Ni	Si	Mn	Mo	Cu	C	P	S	Fe
GM-308L wire	19.5–21	9.0–11.0	0.30–0.65	1.0–2.5	0.50 max	0.75 max	0.03 max	0.03 max	0.03 max	Balance
Built 308L wall	19.86	9.84	0.48	1.70	0.0096	0.076	0.021	0.028	0.019	Balance

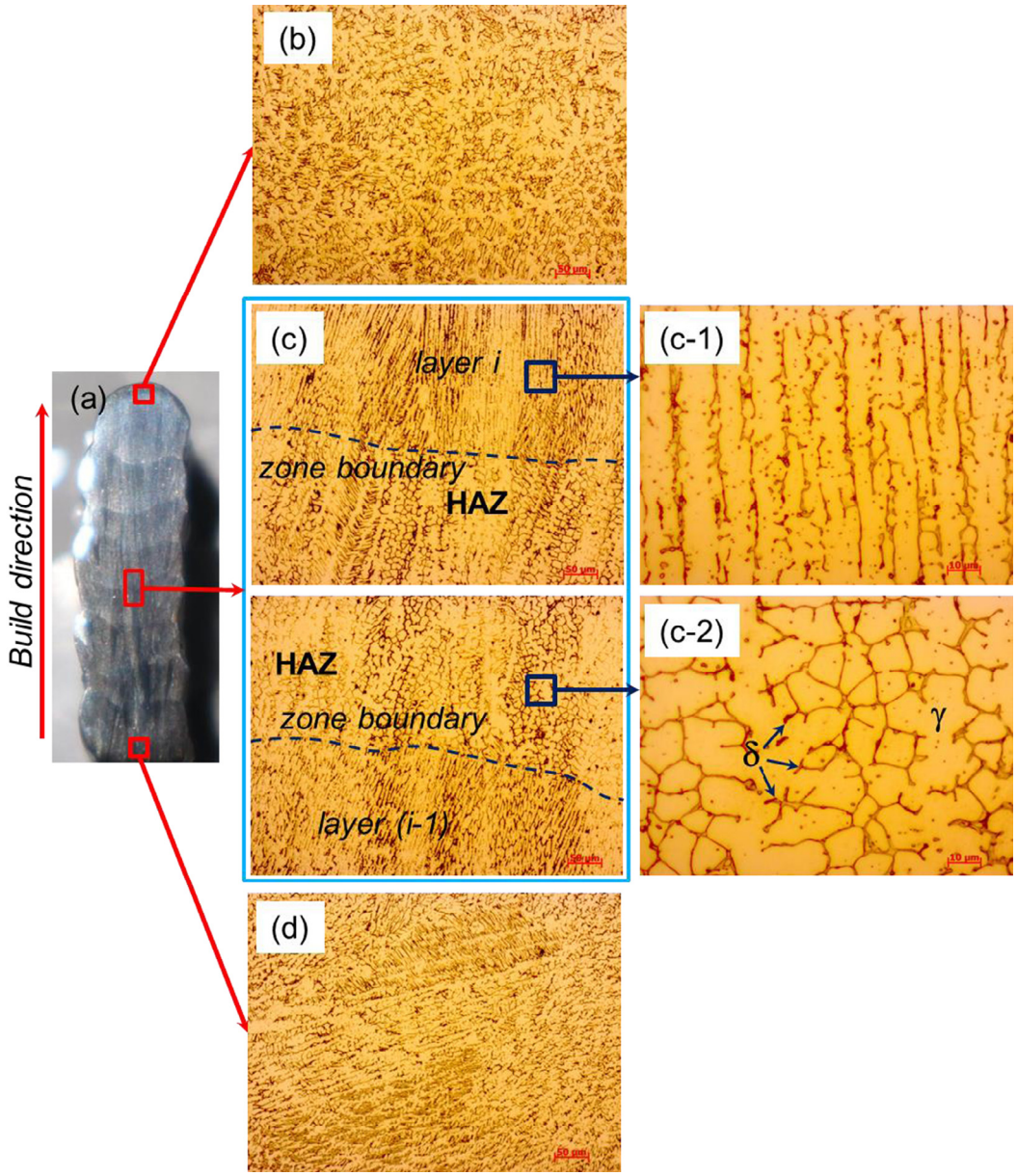

Fig. 1. Microstructures of GMAW-AM thin-walled 308L: (a) overall structure of cross section, (b) the top region, (c) the middle region, (d) the bottom region, (c-1) high magnification photographs of layer *i* and the HAZ between layers *(i-1)* and *i*.

the cross section reveals distinguished wavy bands with well-metallurgical bonding between adjacent layers, and large numbers of columnar dendrites growing along the build direction.

The microstructure of GMAW-AM thin-walled 308L mainly consists of two phases: a small amount of δ ferrite phases displayed within γ austenite dendrites. For austenitic stainless steels, the mode of solidification is determined by the ratio between the chromium equivalent (Cr_{eq}) and nickel equivalent (Ni_{eq}), where Cr_{eq} and Ni_{eq} are calculated by Schaeffler formula [10]: Cr_{eq} = Cr + Mo + 1.5Si + 0.5Nb and Ni_{eq} = Ni + 30C + 0.5Mn. Using the chemical composition of GMAW-AM thin-walled 308L given in Table 1, the values of Cr_{eq} and Ni_{eq} are equal to 20.59% and 11.32% respectively, and the ratio Cr_{eq}/Ni_{eq} = 1.82. In this case, $1.48 < Cr_{eq}/Ni_{eq} < 1.95$, so the GMAW-AM 308L solidifies according to the FA mode [10]: $L \rightarrow L + \delta \rightarrow L + \delta + \gamma \rightarrow \delta + \gamma \rightarrow \gamma$, where L, δ and γ are liquid, delta ferrite and austenite, respectively. The δ ferrite phase is first generated as primary phase. The austenite phase subsequently forms, grows, and gradually replaces the primary ferrites due to the rapid cooling and solidification. The remaining ferrite exists in the grain and sub-grain boundaries of an austenite matrix with vermicular or skeletal structures (e.g. Fig. 1c, c-1, and c-2) or lathy dendrites (e.g. Fig. 1b and d).

Due to the different conditions and thermal cycles, the microstructure of GMAW-AM thin-walled 308L vary along the build direction of the wall. The bottom region reveals columnar dendrites (Fig. 1d) growing in different directions. The microstructure is also finer than other regions, because the heat is directly conducted to the substrate at room temperature, so the cooling rate is higher. The middle region presents typical microstructures of the wall, consisting of vertically-oriented columnar dendrites (Fig. 1c). In this region, the material of the previous layer (i-1) is re-melted by the heat of the successive layer i, generating equiaxed grains in the head affected zone (HAZ) between two adjacent layers (Fig. 1c-2). The grain size in the HAZ is coarser when compared to those in the non-HAZ (Fig. 1c-1). The microstructure of the middle region is coarser than that in the bottom, because when the deposits increase, the heat is accumulated and the cooling rate is slower. The top region contact directly with the air and the time is also short, so it is composed of randomly oriented equiaxed grains (Fig. 1b).

Fig. 2 shows the average microhardness of GMAW-AM thin-walled 308L measured in three regions. In each region, the hardness was measured at four positions distributing on the centerline of the cross section. The average hardness value in the bottom, the middle, and the top region are 169 ± 5.67 ($HV_{0.1}$), 163 ± 5.36 ($HV_{0.1}$) and 155 ± 1.20 ($HV_{0.1}$), respectively. The variation of microhardness is consistent with the observation of microstructures. The microhardness presents the highest average value in the bottom region because the microstructure in this region is finer than that in other regions (Fig. 1).

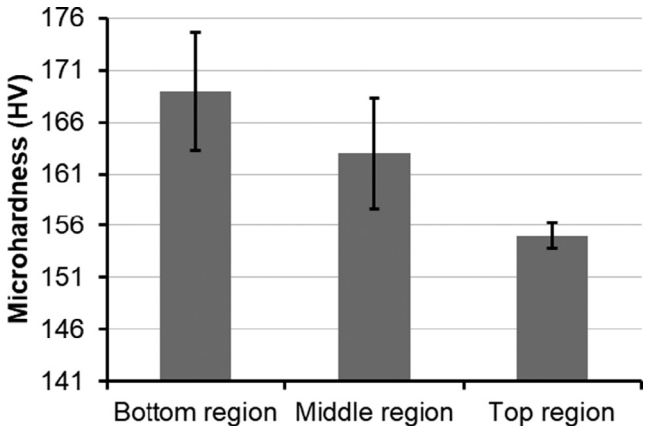

Fig. 2. Microhardness of GMAW-AM thin-walled 308L.

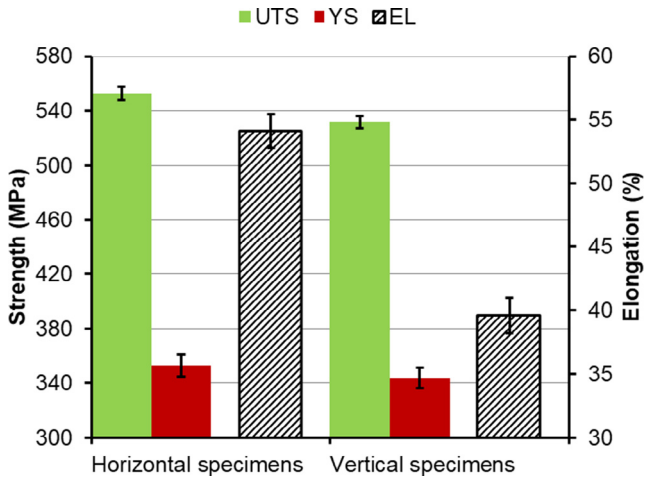

Fig. 3. Tensile properties of thin-walled 308L stainless steel manufactured by the GMAW-AM process.

The ultimate tensile strength (UTS), yield strength (YS) and elongation (EL) of GMAW-AM 308L in both the vertical and horizontal directions are shown in Fig. 3. The average UTS, YS and EL of the built material in the horizontal direction are 552.95 ± 4.96 MPa, 352.69 ± 8.12 MPa, and 54.13 ± 1.29%, respectively, which are obviously higher than those of the vertical specimens (UTS: 531.78 ± 4.52 MPa, and YS: 343.67 ± 7.53 MPa EL: 39.58 ± 1.38%). This is due to the inhomogeneity of microstructures of the built material that is commonly observed in the materials manufactured by WAAM processes.

4. Conclusions

In this study, the thin-walled 308L stainless steel was successfully built by the GMAW-AM process. The metallurgical and mechanical properties of GMAW-AM thin-walled 308L were investigated. The main obtained results can be summarized as follows:

- The microstructure of GMAW-AM thin-walled 308L steel was typically characterized by columnar dendrites in the bottom and middle regions of the wall. The top region of the wall is mainly composed of equiaxed dendrites. The equiaxed grains are also observed in the heat affected zone between two adjacent layers. The microstructure of GMAW-AM thin-walled 308L is composed of small amount of δ ferrite phases existing within γ austenite dendrites.
- The microhardness of GMAW-AM thin-walled 308L steel ranges from 155 to 169 $HV_{0.1}$. The average microhardness of the middle region of the walls is around 163 $HV_{0.1}$.
- The tensile properties of GMAW-AM thin-walled 308L steel present anisotropic characteristics: UTS = 552.95 ± 4.96 MPa, YS = 352.69 ± 8.12 MPa, and elongation = 54.13 ± 1.29% in the horizontal direction, whereas UTS = 531.78 ± 4.52 MPa, YS = 343.67 ± 7.53 MPa, and elongation = 39.58 ± 1.38% in the vertical direction.

Declaration of Competing Interest

The authors declare that they have no known competing financial interests or personal relationships that could have appeared to influence the work reported in this paper.

Acknowledgement

This research is funded by Vietnam National Foundation for Science and Technology Development (NAFOSTED) under grant number 107.99-2019.18.

References

[1] M. Dinovitzer, X. Chen, J. Laliberte, X. Huang, H. Frei, Effect of wire and arc additive manufacturing (WAAM) process parameters on bead geometry and microstructure, Addit. Manuf. 26 (2019) 138–146, https://doi.org/10.1016/j.addma.2018.12.013.

[2] Z. Qi, B. Qi, B. Cong, R. Zhang, Microstructure and mechanical properties of wire + arc additively manufactured Al-Mg-Si aluminum alloy, Mater. Lett. 233 (2018) 348–350, https://doi.org/10.1016/j.matlet.2018.09.048.

[3] B. Wu, Z. Pan, D. Ding, D. Cuiuri, H. Li, J. Xu, J. Norrish, A review of the wire arc additive manufacturing of metals: properties, defects and quality improvement, J. Manuf. Process. 35 (2018) 127–139, https://doi.org/10.1016/j.jmapro.2018.08.001.

[4] V.T. Le, A preliminary study on gas metal arc welding-based additive manufacturing of metal parts, Sci. Technol. Dev. J. 23 (2020) 422–429, https://doi.org/10.32508/stdj.v23i1.1714.

[5] L. Wang, J. Xue, Q. Wang, Correlation between arc mode, microstructure, and mechanical properties during wire arc additive manufacturing of 316L stainless steel, Mater. Sci. Eng. A. 751 (2019) 183–190, https://doi.org/10.1016/j.msea.2019.02.078.

[6] C.V. Haden, G. Zeng, F.M. Carter, C. Ruhl, B.A. Krick, D.G. Harlow, Wire and arc additive manufactured steel: tensile and wear properties, Addit. Manuf. 16 (2017) 115–123, https://doi.org/10.1016/j.addma.2017.05.010.

[7] X. Chen, J. Li, X. Cheng, B. He, H. Wang, Z. Huang, Microstructure and mechanical properties of the austenitic stainless steel 316L fabricated by gas metal arc additive manufacturing, Mater. Sci. Eng. A. 703 (2017) 567–577, https://doi.org/10.1016/j.msea.2017.05.024.

[8] O. Yilmaz, A.A. Ugla, Microstructure characterization of SS308LSi components manufactured by GTAW-based additive manufacturing: shaped metal deposition using pulsed current arc, Int. J. Adv. Manuf. Technol. 89 (2017) 13–25, https://doi.org/10.1007/s00170-016-9053-y.

[9] M. Li, T. Lu, J. Dai, X. Jia, X. Gu, T. Dai, Microstructure and mechanical properties of 308L stainless steel fabricated by laminar plasma additive manufacturing, Mater. Sci. Eng. A. 770 (2020), https://doi.org/10.1016/j.msea.2019.138523 138523.

[10] J.W. Fu, Y.S. Yang, J.J. Guo, J.C. Ma, W.H. Tong, Microstructure evolution in AISI 304 stainless steel during near rapid directional solidification, Mater. Sci. Technol. 25 (2009) 1013–1016, https://doi.org/10.1179/174328408X317093.